

Microstructure and properties of HfC and TaC-based ceramics obtained by ultrafine powder

L. Silvestroni^{a,*}, A. Bellosi^a, C. Melandri^a, D. Sciti^a, J.X. Liu^b, G.J. Zhang^b

^a CNR-ISTEC, National Research Council, Institute of Science and Technology for Ceramics, Via Granarolo 64, I-48018 Faenza, Italy

^b State Key Laboratory of High Performance Ceramics and Superfine Microstructures, Shanghai Institute of Ceramics, 1295 Dingxi Road, 200050 Shanghai, PR China

Received 17 September 2010; received in revised form 18 October 2010; accepted 30 October 2010

Available online 30 November 2010

Abstract

HfC and TaC-based ceramics were hot pressed at 1900 °C for 5–20 min starting from synthesized ultrafine powders. The addition of 5 vol.% of MoSi₂ improved the densification, which increased from around 85–90% for the pure matrices to 95% for the composites. The flexural strength was measured at room temperature and at 1500 °C under protective atmosphere. The added value of this work consists in the utilization of cheap synthesized powders for the realization of the composites with properties comparable to those obtained using more expensive commercial powders. The effect of the nanometric size of the starting powder showed to have the potential to improve the densification behavior and the mechanical properties, however it is necessary a further optimization of the synthesis condition in order to avoid the formation of agglomerates of unreacted powder.

© 2010 Elsevier Ltd. All rights reserved.

Keywords: Hafnium carbide; Tantalum carbide; Hot pressing; Microstructure; Mechanical properties

1. Introduction

Tantalum carbide and hafnium carbide are considered candidates for extremely high-temperature applications in view of their high melting point (>3900 °C), high hardness, elastic modulus and resistance to chemical attack.^{1–3} Proposed uses include rocket nozzles and scramjet components, where the operating temperatures can be in excess of 3000 °C. Monolithic TaC or HfC are traditionally difficult to densify due to their highly covalent bonds and low self-diffusion coefficients. Therefore, hot pressing has been typically used to enhance the densification of these compounds. Several studies report the results of attempts to improve the densification of carbides since the 1960s. TaC was densified up to 90–95% by hot pressing, at temperatures in the range 2200–3000 °C.^{4–6} Other studies report that the temperature needed for densification was strongly reduced (1400–1800 °C) with small amounts of Fe, Mn, Co and Ni.^{7,8} Recently, it has been demonstrated that the addition of C and B₄C enhance the densification of TaC.^{9,10}

These additives are believed to favor the elimination of the surface oxides present on the starting particles. Similar densification problems were encountered for hafnium carbide. Opeka et al. sintered HfC_x compounds by hot pressing at 2500 °C, achieving materials with mean grain sizes of the order of ~40–60 μm.^{11,12} Lack of control of the microstructure, due to grain coarsening and entrapped porosity, is thus the main issue for these compounds. Sciti et al. densified HfC and TaC based materials by hot pressing using TaSi₂ or MoSi₂ as sintering aid.¹³ Optimization of sintering conditions and microstructural parameters led to the following mechanical properties: flexural strength ranging from 670 to 900 MPa for TaC-based and 410–460 MPa for HfC-based composites. The fracture toughness measured by the Chevron notched beam in flexure was 4.7 and 3.8 MPa m^{1/2} for TaC and HfC-based composites, respectively. The Young's modulus ranged from 450 to 490 GPa. HfC-based composites were also pressureless sintered at 1950 °C adding 5–20 vol.% MoSi₂.¹³ For these materials, values of mechanical strength were 450–465 MPa, the elastic modulus was in the range 415–434 GPa and the fracture toughness measured by the CNB method was found to be 3.5–3.6 MPa m^{1/2}.¹³ By pressureless sintering or spark plasma sintering, HfC-based composites were densified at

* Corresponding author.

E-mail address: laura.silvestroni@istec.cnr.it (L. Silvestroni).

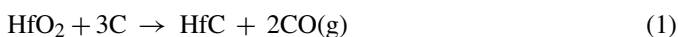
1900–1950 °C with amounts comprised between 3 and 20 vol.% of molybdenum silicide achieving fine microstructures with grain size of the order of few micrometers (1–3 μm).^{14,15}

In this work, the densification, microstructure and mechanical properties of TaC- and HfC-monoliths and composites containing 5 vol% MoSi₂, produced starting from synthesized ultrafine powders, are presented and discussed. The main novelty of this work is the use of synthesized near nanometric powders. The effect of starting powder characteristics is also investigated.

2. Experimental

2.1. Powder synthesis

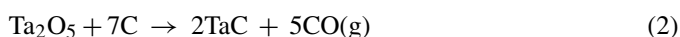
For the synthesis of HfC powders, Hafnium dioxide, HfO₂ (purity >99.5%, main impurities include Zr <0.46%, specific surface area by BET about 11.3 m²/g, mean particle size 100 nm) and carbon black (purity >99.9%, mean particle size about 42 nm, surface area about 75 m²/g) were used as starting powders. HfO₂ and C corresponding to a molar ratio of 1/3 according to reaction (1) were mixed with a rolling ball mill for 24 h, using ethanol and Si₃N₄ balls as mixing solvent and medium, respectively:



Afterwards, the slurry was dried in a rotary evaporator at 80 °C. The powder mixtures was then pressed into disks with diameter of 37 mm under a pressure of 9.8×10^5 Pa in order to improve particle contact for promoting reaction at high temperatures. Finally, the disks were put in a graphite crucible and heat treated in a graphite resistance furnace (ZT-18-22, Shanghai Chenhua Electrical Furnace Inc., Shanghai, China) by two-stage heating process. First, the temperature rose to 1600 °C and was held for 1 h. Then, the samples were continually heated to 1800 °C and soaked at this temperature for 0.5 h. In all the thermal treatments, the heating rate was 16.7 °C/min, while the dynamic initial vacuum in the furnace chamber was kept as low as 5 Pa. Once the furnace had naturally cooled down to room temperature, the disks were lightly crushed in an agate mortar and then sieved through a 200-mesh screen. The purity of the synthe-

sized HfC powder was around 97.9 wt% and the free carbon content was about 0.47 wt% (determined by chemical analysis). The zirconium content was about 0.81 wt% (determined by glow discharge mass spectrometer analysis, VG9000, Thermo Elemental, Cheshire, UK). The oxygen content was <0.72 wt% (determined by oxygen analyzer, TC600, Leco, St. Joseph, MI, USA). The rounded particle morphology of the HfC powder is shown in Fig. 1a. The mean particle dimension was around 225 nm, as determined by SEM analysis.¹⁶

Tantalum pentoxide, Ta₂O₅ (purity >99.9%, particle size about 100 nm) and carbon black (purity >99.9%, particle size about 42 nm, surface area about 75 m²/g) were used as starting powders. Ta₂O₅ and C with mole ratio according to reaction (2) were mixed on a rolling ball mill for 24 h, ethanol and Si₃N₄ balls were used as mixing medium:



Subsequently, the slurry was dried in a rotary evaporator at 80 °C. As for the synthesis of HfC, the powder mixture was dry pressed into disks under a low pressure of 9.8×10^5 Pa. Then, the disks were put in a graphite crucible and heat treated in a graphite resistance furnace (ZT-18-22, Shanghai Chenhua Electrical Furnace Inc., Shanghai, China). TaC powder was synthesized by two-stage heating process: first, the temperature rose to 1200 °C and was held for 3 h. Next, the samples was continually heated to 1400 °C and soaked at that temperature for 0.5 h. In all heating process, the heating rate was 16.7 °C/min, the dynamic vacuum in the furnace chamber was kept by a pump and the initial gas pressure was below 5 Pa. After the furnace cooled naturally to room temperature, the disks were manual crushed lightly into powders in an agate mortar and then sieved through a 200-mesh screen. The purity of the synthesized TaC powder was around 99.5 wt% (determined by chemical analysis) and the oxygen content was <0.49 wt% (determined by oxygen analyzer, TC600, Leco, St. Joseph, MI, USA). The rounded particle morphology of the TaC powder is shown in Fig. 1b. The mean particle dimension was around 250 nm, as determined by SEM analysis, the finest fraction was of the order of 25 nm, the coarsest particles had approximate size of 500 nm.¹⁷

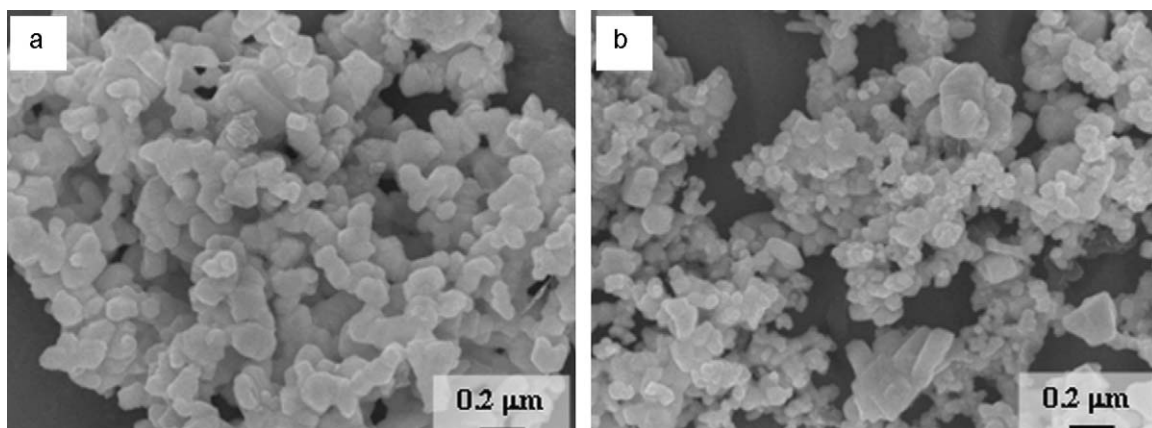


Fig. 1. Synthesized powders: (a) HfC and (b) TaC.

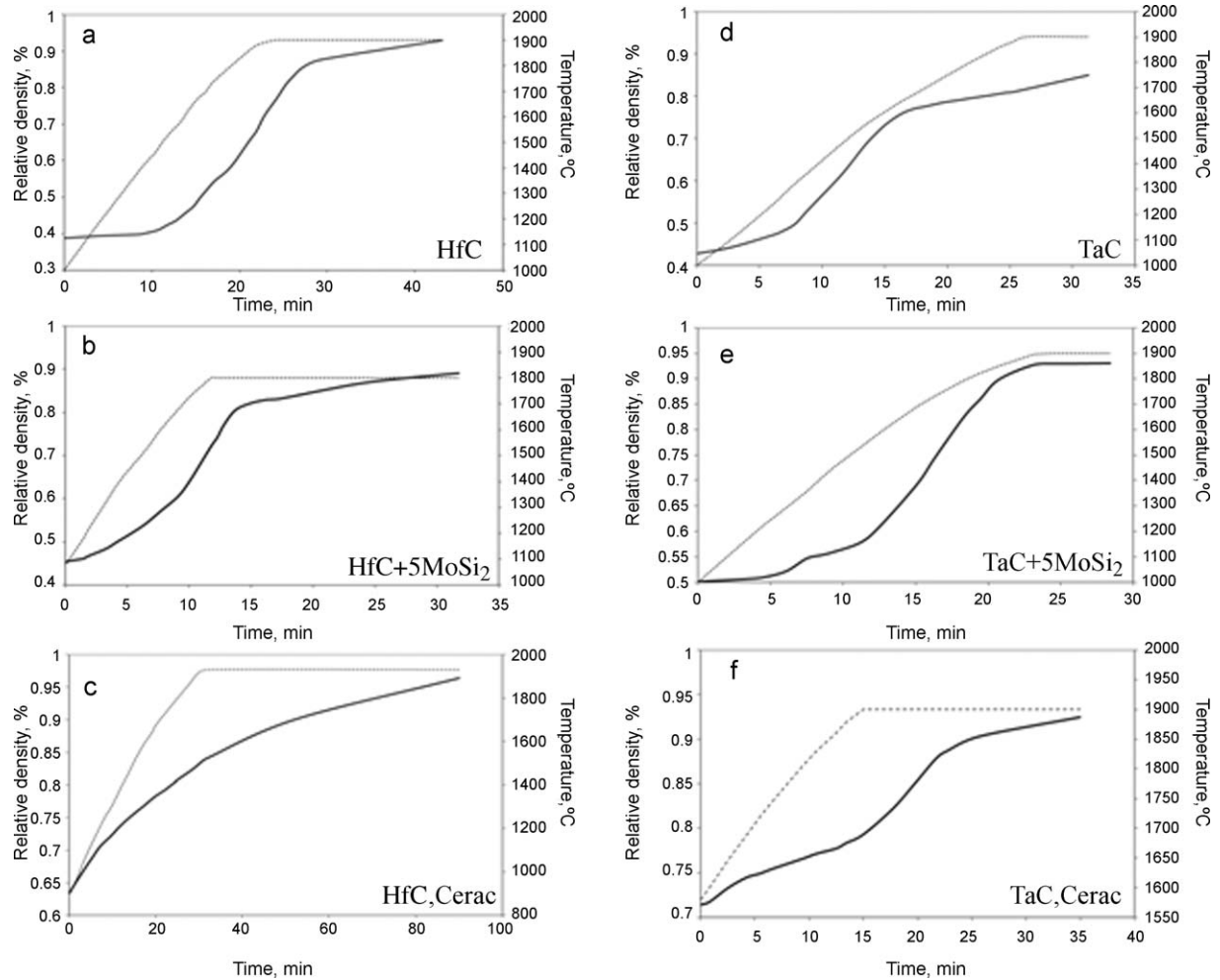


Fig. 2. Densification curves recorded during the hot pressing cycles for (a) pure HfC, (b) HfC + 5 MoSi₂, (c) commercial HfC, (d) pure TaC, (e) TaC + 5 MoSi₂ and (f) commercial TaC.

2.2. Materials preparation

TaC and HfC synthesized powders were compacted by linear uniaxial pressing at 10 MPa and subsequently hot pressed at 1900 °C, with an applied pressure of 30 MPa and holding time 5–20 min in low vacuum (~100 Pa). The linear shrinkage curves for the monoliths are shown in Fig. 2a and d.

The composite materials were obtained by mixing the as-synthesized powders with 5 vol.% of MoSi₂ (<2 μm, Aldrich, USA; mean particle size 2.8 μm, grain size range 0.3–5 μm, oxygen content ~1 wt%), which was previously ball milled in ethanol for 3 days. The powder mixtures were ball mixed for 24 h in absolute ethanol using zirconia milling media. Subsequently the mixtures were dried in a rotary evaporator and sieved through a 60-mesh screen. Hot-pressing was conducted in low vacuum (~100 Pa) using an induction-heated graphite die with a constant uniaxial pressure of 30 MPa, heating rate 20 °C/min and free cooling. For each composition, the same sintering cycle as the monolithic powder was applied to study the effect of the sintering additive. The bulk densities were measured by Archimedes' method, considering as the theoretical density the value obtained from the nominal composition. The linear shrinkage curves for the composites are shown in Fig. 2b and e.

To compare the sinterability of the synthesized powders, pure HfC and TaC materials were densified with the same hot pressing equipment starting from commercial powders (HfC Cerac Inc., Milwaukee, WI, particle size range 0.2–1.5 μm, purity 99.5%, mean particle size 0.7 μm; TaC Cerac Inc., Milwaukee, WI particle size range 0.2–1.5 μm, purity 99.5%). Commercial HfC and TaC were hot pressed at 1930 °C for 60 min and 1900 °C for 20 min, respectively. The linear shrinkage curves for the commercial powder are shown in Fig. 2c and f.

Crystalline phases were identified by X-ray diffraction (Siemens D500, Germany). The microstructures were analyzed using scanning electron microscopy (SEM, Cambridge S360, Cambridge, UK) and energy dispersive spectroscopy (EDS, INCA Energy 300, Oxford instruments, UK) on fractured and polished surfaces. Mean grain sizes, amount of porosity and of secondary phases were determined through image analysis on SEM micrographs of polished surfaces using a commercial software program (Image Pro-plus 4.5.1, Media Cybernetics, Silver Springs MD, USA). At least 100 grains per specimen were measured for the determination of the mean grain size.

Vickers microhardness (H_V 1.0) was measured with a load of 9.81 N, using a Zwick 3212 tester. Young's modulus (E) was calculated from the slope of the load–displacement curves once

subtracted the loading train compliance. Fracture toughness was determined by the indentation crack length method using a diamond indenter with a load of 5 kg for 10 s on a polished surface, using Charles and Evans's formula.¹⁸

The specimens were tested in bending flexure using a semi-articulated silicon carbide four-point fixture with a lower span of 20 mm and an upper span of 10 mm using a screw-driven load frame (Instron mod. 6025). The flexural strength (σ) was measured at room temperature and at 1500 °C on polished and chamfered bars 25 mm × 2.5 mm × 2 mm (length × width × thickness, respectively), using a crosshead speed of 0.5 mm/min. The high-temperature strength was tested at 1500 °C under a flowing argon protective gas. Before the bending test, a soaking time of 18 min was set to reach thermal equilibrium. For each composition, five specimens were tested at room temperature and three specimens at 1500 °C.

3. Results

3.1. Densification behavior

Density data and sintering cycles are summarized in Table 1. Shrinkage curves vs. time are displayed in Fig. 2. All the materials required at least 1900 °C for the densification, for HfC-based ceramics a dwell time at the maximum temperature was set as 20 min, for TaC-based 5 min were enough.

Ultrafine HfC started shrinking at around 1400 °C (Fig. 2a), achieved a maximum densification rate of $3 \times 10^{-2} \text{ min}^{-1}$ (Table 1) at 1800 °C and it reached a bulk density of 11.03 g/cm³, which corresponds to about 89% of the theoretical density. HfC–MoSi₂ started shrinking at a higher temperature, 1540 °C, but achieved a maximum densification rate of $4.6 \times 10^{-2} \text{ min}^{-1}$ (Table 1) at 1800 °C, achieving a final density of 11.80 g/cm³, about 93% (Fig. 2b).

Commercial HfC powder started the densification at 900 °C, achieved a maximum densification rate of $1.1 \times 10^{-2} \text{ min}^{-1}$ at the beginning of the shrinkage (900–1000 °C) and reached a final density of 12.2 g/cm³, about 96%, after a holding temperature at 1930 °C for 60 min (Fig. 2c).

Ultrafine TaC started the densification at 1100 °C, achieved a maximum densification rate of $3.1 \times 10^{-2} \text{ min}^{-1}$ (Table 1) at 1450 °C and after the dwell time, achieved a density of 12.32 g/cm³, that is around 85% of the theoretical value (Fig. 2d). The composite containing MoSi₂, (Fig. 2e) started shrinking at 1000 °C and achieved a maximum densification rate of $4.3 \times 10^{-2} \text{ min}^{-1}$ (Table 1) at 1700 °C and a final density of 13.1 g/cm³, 93% of the final value calculated by the rule of the mixtures. It can be noticed that this composite showed another peak of densification rate between 1300 and 1350 °C of $2.47 \times 10^{-2} \text{ min}^{-1}$, probably due to mechanical powder compacting.

Commercial TaC powder achieved a final density of 13.4 g/cm³ after sintering at 1900 °C for 20 min, this powder started shrinking at around 1570 °C and achieved a maximum densification rate of $1.4 \times 10^{-2} \text{ min}^{-1}$ (Table 1) at 1800 °C (Fig. 2f).

Table 1
Composition, sintering parameters, experimental density, mean grain size of the matrix, Vickers hardness (H_V , 1 kg), fracture toughness (K_{Ic} , 5 kg), flexural strength (σ) at room temperature and at 1500 °C in Ar.

| Label | Composition (vol.%) | Sintering (°C, min, MPa) | Shrink. rate (D/dt, 10 ⁻² min ⁻¹) | Density (g/cm ³) | Density (%) | MGS (μm) | H_V 1.0 (GPa) | K_{Ic} 5 (kg MPam ^{1/2}) | σ_{RT} (MPa) | σ_{1500} (MPa) |
|------------|------------------------|--------------------------|--|------------------------------|-------------|----------|-----------------|--------------------------------------|---------------------|-----------------------|
| HfC | HfC | 1900, 20, 30 | 3.0 | 11.03 | 89 | 0.33 | 5.79 ± 0.61 | 1.88 ± 0.15 | 352 ± 8 | 301 ± 15 |
| HfCM | HfC+5MoSi ₂ | 1900, 20, 30 | 4.6 | 11.80 | 93 | 1.9 | 17.84 ± 1.45 | 2.94 ± 0.15 | 429 ± 97 | 406 ± 26 |
| HfC, Cerac | HfC | 1930, 60, 30 | 1.1 | 12.23 | 96 | 20–30 | – | – | – | – |
| TaC | TaC | 1900, 5, 30 | 3.1 | 12.32 | 85 | 0.8 | 11.14 ± 0.77 | 2.60 ± 0.17 | 376 ± 8 | 257 ± 41 |
| TCM | TaC+5MoSi ₂ | 1900, 5, 30 | 4.3 | 13.11 | 94 | 2.8 | 13.69 ± 0.35 | 3.45 ± 0.26 | 585 ± 5 | 308 ± 41 |
| TaC, Cerac | TaC | 1900, 20, 30 | 1.4 | 13.41 | 92 | 20 | – | – | – | – |

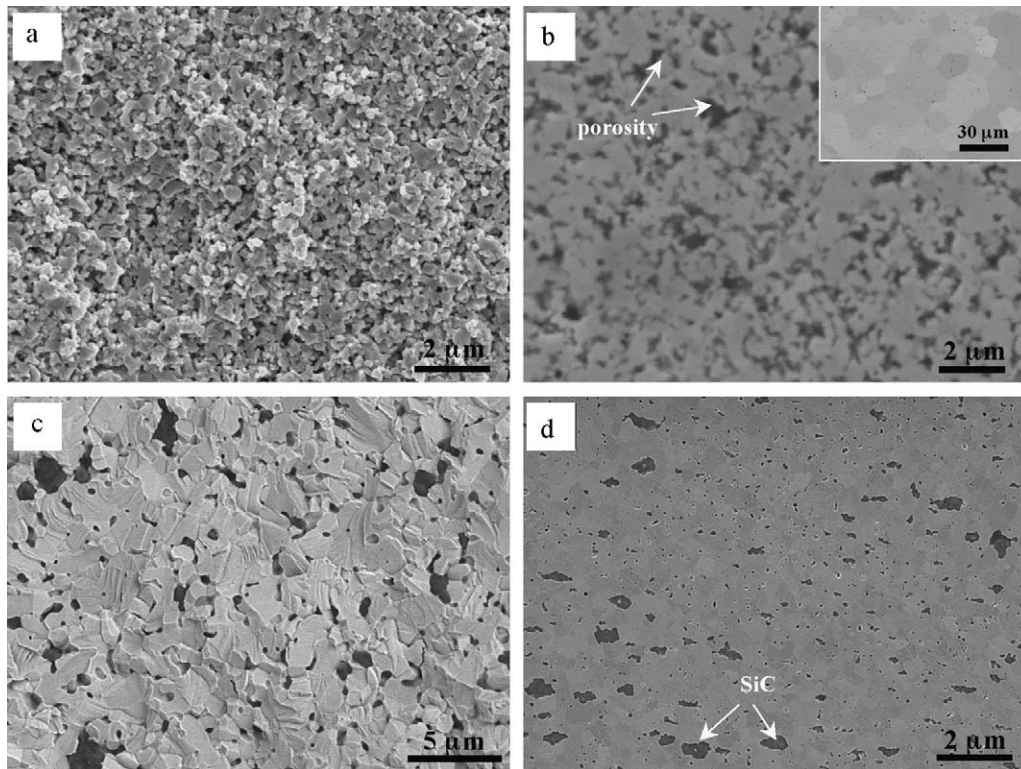


Fig. 3. Fracture and polished surface for (a) and (b) pure HfC, and (c) and (d) HfC + 5 MoSi₂, respectively. The inset in (b) is the polished surface of hot pressed commercial HfC powder.

In Table 1, the shrinkage rate of the ultrafine monoliths, of the composites and of the two pure commercial powders is also reported for comparison. Concerning HfC-based ceramics, the slowest shrinkage rate belongs to commercial HfC, followed by the synthesized HfC powder and the fastest is the HCM composite. Analogous trend is observed for TaC-based ceramics, which possess a higher rate than the corresponding HfC-powders, despite similar mean grain size.

3.2. Microstructure

3.2.1. HfC-based materials

The microstructure of the two HfC-based materials produced with ultrafine powder is presented in Fig. 3. As far as the pure HfC is concerned, it is well evident, both from the fracture surface and from the polished section (Fig. 3a and b), that a notable amount of residual porosity is still present even after the sintering at 1900 °C. The fracture surface (Fig. 3a) shows that densification is at an early stage. The particles are still separated, even at higher magnification necks were barely visible and the mean grain size is of the same order of the starting powder. From image analysis the dark phase in Fig. 3b was estimated to be around 10 vol.%, which is in agreement with the density obtained by Archimedes' method. The inset in Fig. 3b shows the polished section of the commercial HfC material. In this case the porosity, recognizable as rounded black areas, was calculated to be below 5%, but the grain size increased up to 20–30 μm.

On the other hand, HCM sample in Fig. 3c and d shows a denser microstructure with a residual porosity calculated by image analysis to be less than 5 vol.%. The bright phase is HfC, the dark phase is SiC, which formed after reduction of the SiO₂ covering MoSi₂ particles by the reducing sintering environment. MoSi₂ is barely detectable in the final microstructure and it is recognizable as grey phase, often close to SiC particles, as illustrated in Fig. 4. In addition, SiO₂ pockets and (Hf,Mo)₅Si₃ phase were observed, in agreement with analogous HfC-based materials.¹⁹ The crystalline phases identified by X-ray diffraction were cubic HfC and traces of MoSi₂.

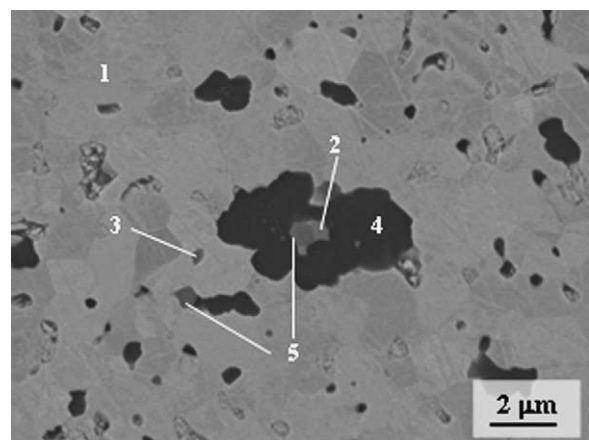


Fig. 4. Enlarged view of the HCM composite showing the secondary phases. Legend: 1 – HfC, 2 – MoSi₂, 3 – SiO₂, 4 – SiC, 5 – (Hf,Mo)₅Si₃.

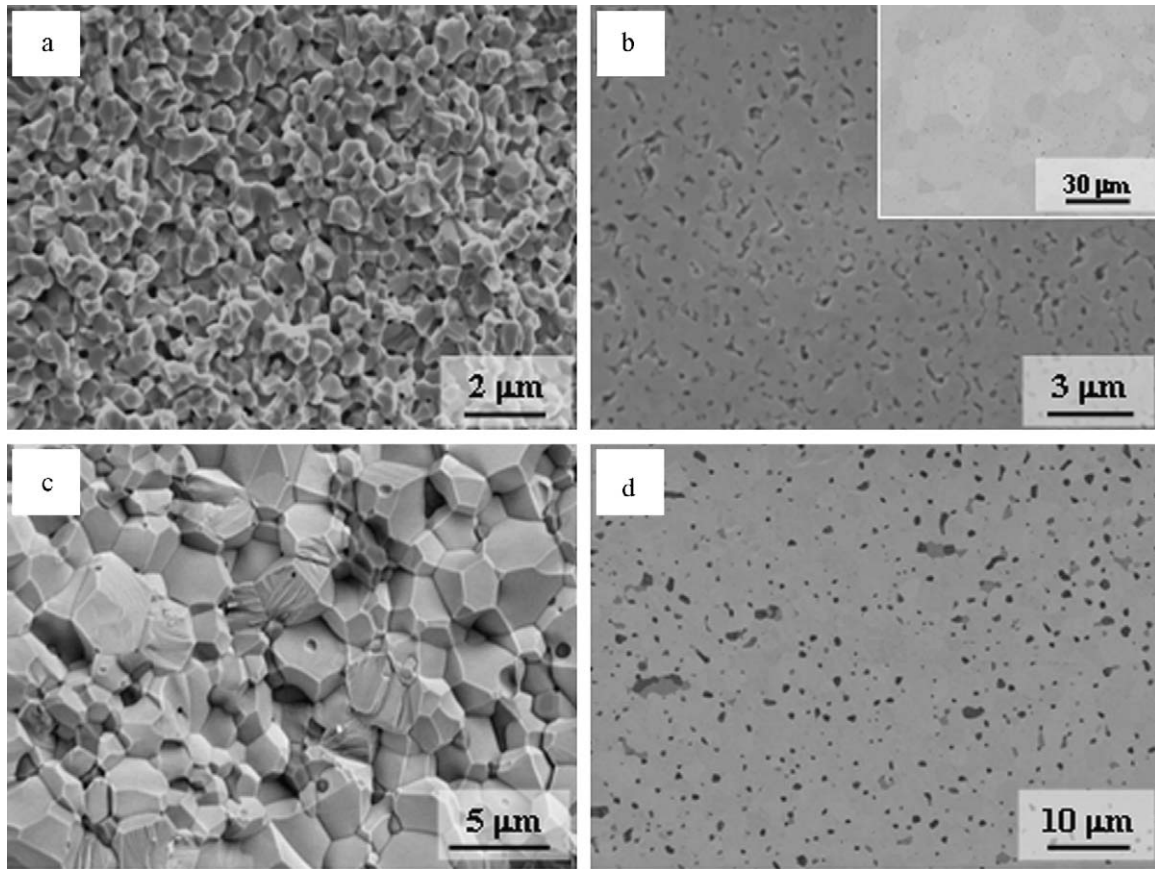


Fig. 5. Fracture surface and polished surface for (a) and (b) pure TaC and (c) and (d) TaC + 5 MoSi₂, respectively. The inset in (b) is the polished surface of hot pressed commercial TaC powder.

3.2.2. TaC-based materials

The monolithic TaC material had a final density of 12.32 g/cm³, that corresponds to 85% of relative density. The presence of a high amount of open porosity is apparent in the micrograph displayed in Fig. 5a and b and the mean particle size is still lower than 1 μm. In the inset of Fig. 5b the polished section of a sintered specimen obtained with commercial TaC powder is illustrated for comparison. A denser, but coarser microstructure with grains as large as 20 μm is visible, the black areas are trapped porosity mainly located within the grains.

When 5 vol.% of MoSi₂ was added, there was a notable increase of the final density, which reached a nominal value of 93% of the theoretical value. The X-ray diffraction pattern gave evidence only for cubic TaC, no traces of MoSi₂ were detected after sintering. The fractured and polished sections of TCM (Fig. 5c and d) show that this composite has an homogeneous microstructure. The TaC matrix grains in the polished surface has a squared shape and are quite homogeneous in size, around 3 μm. MoSi₂ appears as irregularly shaped phases with very low dihedral angles, indicating its ductile behavior at the sintering temperature. In the apical part of MoSi₂, at the interface with the matrix, a mixed phase was observed with composition close to (Mo,Ta)₅Si₃ (Fig. 6). Despite the low value of relative density, little porosity was detected by SEM. The discrepancy between SEM observation and the relative density value reported in Table 1 is due to a considerable amount of silica pockets in the

microstructure, about 2–3 vol.%, as verified by image analysis. SiO₂ contamination has been already observed in all the composites containing MoSi₂ as secondary phase.¹³ Large pockets of SiC were also detected by SEM–EDS analysis (Fig. 6).

3.3. Mechanical properties

The values of the mechanical properties are summarized in Table 1. For pure HfC, porosity seems to affect hardness and

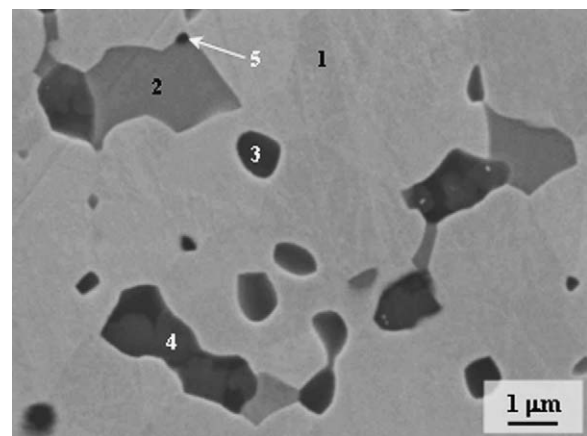


Fig. 6. Enlarged view of the TCM composite showing the secondary phases. Legend: 1 – TaC, 2 – MoSi₂, 3 – SiO₂, 4 – SiC, 5 – (Mo,Ta)₅Si₃.

fracture toughness more than flexural strength. It is worthy to note that the strength tested at 1500 °C in Argon atmosphere is not very different from the room temperature value for both the HfC-based ceramics (352 and 301 MPa for pure HfC, 429 and 406 MPa for HCM at room temperature and at 1500 °C, respectively). For the composite HCM, the increase of the final relative density induced an improvement for all the properties. The large deviation displayed by the strength values is due to the presence of large defects, which are mainly residual agglomerates of unreacted HfO₂ (Fig. 7). These HfO₂ inclusions were randomly distributed, indicating that the green shaping was optimized. No MoSi₂-agglomerates were identified to act as critical defects, thanks to the accurate powder processing.

All the properties of the TaC-based composite, TCM, improved in comparison with the monolith, due to the reduction of the residual porosity. Both hardness and fracture toughness increased and the room temperature strength increased of about 35% compared to the monolith.

The surface of the samples after bending test at 1500 °C in Argon is reported in Fig. 8. Despite flushing the chamber with Ar, contact with oxygen species was not completely avoided. As a consequence, an oxidation layer formed on the surfaces for all the carbides. The surface of the monolith HfC (Fig. 8a) was completely covered by HfO₂, which looked porous and quite rough. For HCM, addition of MoSi₂ (Fig. 8b) resulted in formation a silica-based glassy phase, due oxidation of the silicide. In

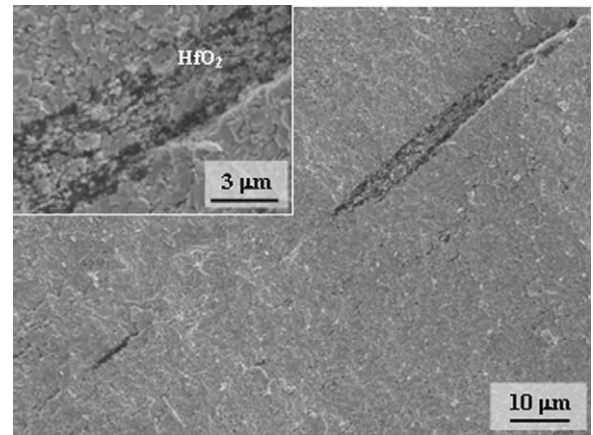


Fig. 7. Example of critical flaw in the pure HfC sample after room temperature bending test. In the inset an enlargement of the HfO₂ defect.

Fig. 8c the surface of pure TaC is presented. The bright Ta₂O₅ platelets were immersed in a oxygen-deficient tantalum oxide phase (EDS in Fig. 8c) which had a ductile aspect, the scale was compact and the platelets were homogeneously distributed. It seems that the addition of MoSi₂ hinders the development of such Ta₂O₅ grains, as in Fig. 8d they were not visible, but the surface is constituted by ~3 μm agglomerates of smaller Ta–O particles covered by a glassy SiO₂-based glassy layer. Little

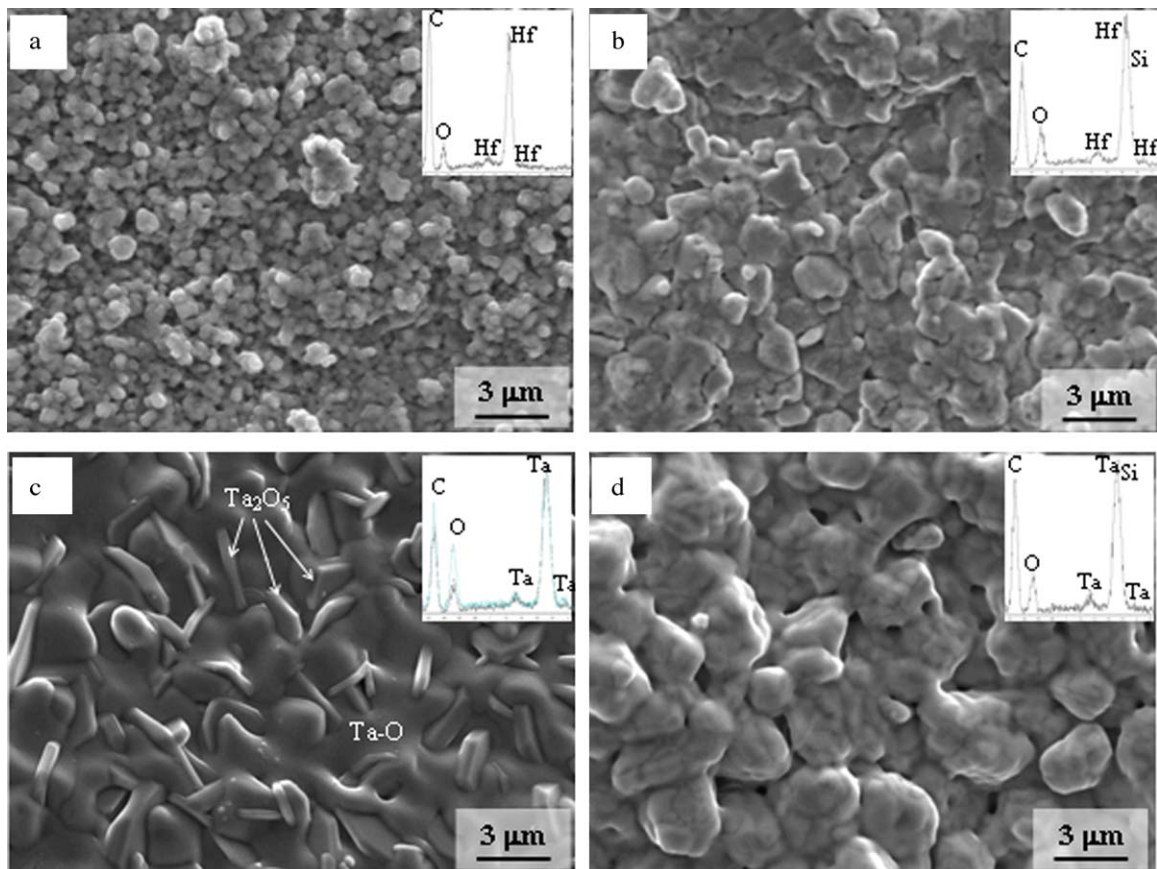
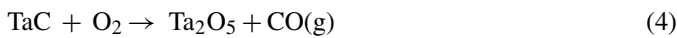
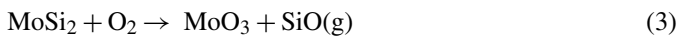


Fig. 8. Fracture surface after bending tests at 1500 in Ar environment of (a) pure HfC, (b) HCM5, (c) pure TaC and (d) TCM5 sample with the corresponding EDS spectra. The high C peak derives from carbon coating.

Table 2
Comparison among HfC- and TaC-based ceramics. Composition, sintering parameters, final relative density, mean grain size, Vickers hardness (1 kg), 4-pt flexural strength at room temperature and at 1500 °C in argon atmosphere.

| Composition (vol.%) | Sintering (°C, min, MPa) | Rel. density (%) | mgs (μm) | H_V 1.0 (GPa) | σ_{RT} (MPa) | σ_{1200} (MPa) | σ_{1500} (MPa) | Ref. |
|----------------------------|--------------------------|------------------|----------|-----------------|---------------------|-----------------------|-----------------------|--------------|
| Pure HfC | HP 1900, 20, 30 | 93 | 0.33 | 5.79 ± 0.61 | 352 ± 8 | – | 301 ± 15 | Present work |
| HfC, Cerac | HP 1930, 60, 35 | 96.3 | 20–30 | – | – | – | – | Present work |
| HfC, Cerac | SPS 2200, 3, 65 | 98.0 | 19 | 18.3 ± 0.5 | 467 ± 7 | – | – | 14 |
| HfC + 1MoSi ₂ | SPS 1900, 5, 100 | 98 | 2.2 | 21.1 ± 0.7 | – | – | – | 14 |
| HfC + 3MoSi ₂ | SPS 1750, 5, 100 | 99.7 | 0.9 | 22.2 ± 0.7 | 868 ± 92 | – | – | 14 |
| HfC + 5MoSi ₂ | HP 1900, 20, 30 | 89 | 1.9 | 17.84 ± 1.45 | 429 ± 97 | – | 406 ± 26 | Present work |
| HfC + 5MoSi ₂ | PLS 1950, 60, – | 98 | 4 | 15.6 ± 0.6 | 465 ± 45 | 404 ± 31 | 241 ± 112 | 15 |
| HfC + 15MoSi ₂ | HP 1900, 10, 30 | 98.6 | 1.2 | 19.6 ± 0.5 | 417 ± 38 | 294 ± 39 | – | 13 |
| Pure TaC | HP 1900, 5, 30 | 85 | 0.8 | 11.14 ± 0.77 | 376 ± 8 | – | 257 ± 41 | Present work |
| TaC, Cerac | HP 1900, 20, 30 | 92 | 15 | – | – | – | – | Present work |
| TaC, Atlantic equipment | HP 2300, 60, 30 | 94.3 | 1.6 | 14.1 ± 0.2 | 690 ± 60 | – | – | 10 |
| TaC + 10.5B ₄ C | HP 2100, 60, 30 | 99 | 1.5–3 | 16.3 | 550 ± 50 | – | – | 10 |
| TaC + 5MoSi ₂ | HP 1900, 5, 30 | >94 | 2.8 | 13.69 ± 0.35 | 585 ± 5 | – | 308 ± 41 | Present work |
| TaC + 15MoSi ₂ | HP 1850, 3, 30 | 96.3 | 1.2 | 14.5 ± 0.3 | 900 ± 33 | 537 ± 45 | – | 13 |

porosity is also visible and may be the result of gases escape generated by processes like those described by Reactions (3) and (4):



which are active oxidation reactions occurring when carbon sources are available even if the testing environment is backfilled with Argon.¹³

Generally speaking, HfC-based composites have higher values of hardness (17.8 GPa), but lower toughness and strength (2.9 MPam^{1/2} and 430–350 MPa) than TaC-based materials (13 GPa, 3.45 MPam^{1/2} and 585 MPa, respectively). However the latter system shows a higher decrease of strength with increase of the test temperature, due to oxidation damage.

4. Discussion

The densification data confirm what is a general behavior of the ultra-refractory carbides. Temperature well over 2000 °C are necessary to obtain fully dense pure HfC and TaC materials. For instance, in an earlier work, pure HfC was fully densified by spark plasma sintering at a nominal temperature of 2200 °C, with a final relative density of 98% and mean grain size approaching 20 μm (powder purity 99.5%, mean particle size 0.7 μm).¹⁴ It is generally recognized that fine powders have a higher sinterability compared to coarser ones due to the higher specific surface area, which in turn increases the particles reactivity. The use of finer powder particles, as those of the present work (~225–250 nm), does increase the shrinkage rate, as Table 1 evidences, but does not allow the achievement of a full densification even at 1900 °C. From this point of view, the final densities obtained with ultrafine powders are not significantly improved in comparison with the commercial powders.

Several reasons may explain this unexpected behavior: on one hand, the finer is the powder particles, the more difficult is to obtain a good compaction without specific powder treatments,

such as granulation. Indeed, from the sintering curves in Fig. 2, it can be noticed that the commercial powders (Fig. 2c and f) started the sintering cycle at a higher relative density, 65–70%, compared to the ultra-fine powders, 35–50%, despite they were uniaxially pressed at the same pressure before the hot pressing treatment.

Secondly, it is believed that inhibition of sintering in ultra-refractory carbides is attributed to the presence of oxide impurities on the powder particle surface.⁹ The lowest degree of purity of the synthesized powders suggests a higher level of contamination from residual oxides which can be very detrimental for densification. Baik and Becher reported indeed that more than 0.5 wt% of oxygen contamination inhibited the densification of TiB₂, favoring grains coarsening.²⁰ Furthermore, the higher is the specific surface area, the higher is the possibility to get oxygen contamination during powder processing.

Problems are not fully overcome when a sintering aid such as MoSi₂ is added. Although, the addition of MoSi₂ certainly improved the densification behavior, comparison with previous works demonstrates that the efficacy of this sintering aid was reduced. The final density of the composites HCM, TCM was still well below the theoretical value and lower than density values previously obtained for commercial carbides doped with different level of MoSi₂.^{10,13–15} A collection of data from previous works can be found in Table 2. One possible explanation is the difficulty to obtain an intimate mixing between ultrafine carbide powders (200–300 nm) and micrometer disilicide powders (3 μm), due to the difference in mean particle size. The non-homogeneous distribution of the additive probably resulted in non-homogeneous shrinkage which in turn determined formation of critical flaws such as residual porosity or agglomerations.

In theory, materials produced from ultrafine powders have the potential to become ceramics with refined microstructure and thus to possess improved mechanical properties. However, the results here presented show that the non-optimized control of the starting powder characteristics, in term of purity, and non-optimized powder processing nearly jeopardized the potential

advantages of ultrafine powders. Indeed, even if the microstructure is refined, processing defects (porosity or agglomerations) may have dimensions two or three orders of magnitude higher than those of the starting particles (see Fig. 7). The consequence of this was that the mechanical properties of ultrafine carbides were not superior that those displayed by other TaC and HfC composites realized with MoSi₂. Similar problems were already encountered with the use of other submicrometric or nanometric powders in processing of SiC-based materials.²¹

The direct comparison of some previously produced HfC- or TaC-based materials, in Table 2, reveals the potential of carbides produced from ultrafine powders. For the hardness, the refinement of microstructure was counterbalanced by residual porosity. The strength of HfC derived from the nano-carbide powder was 429 MPa, that is in the range of other HfC-based materials,^{13–15} but could be increased by reducing the porosity in the final ceramic. Noteworthy, at 1500 °C the HCM maintained this value unchanged, differently from a pressureless sintered HfC,¹⁵ which halved the strength.

Pure TaC hot pressed at 2300 °C¹⁰ resulted in a fully dense material possessing a strength of 690 MPa, compared to ultrafine TaC obtained in the present work, 376 MPa. The composite TCM of the present work displayed a room temperature strength in the range of other TaC-based ceramics,¹⁰ around 600 MPa.

This work points out that the utilization of synthesized ultrafine powder to produce hafnium and tantalum carbide composites can be a strategy to obtain material in a cheaper way, possessing good mechanical properties, once the green forming and the sintering cycle are optimized.

5. Conclusions

Ultrafine powder were used for the production of HfC and TaC-based ceramics. Pure powders and with 5 vol.% of MoSi₂ were hot pressed at 1900 °C for 5–20 min with an applied pressure of 30 MPa. The monolith HfC and TaC had a final density of 85–90%, while the addition of MoSi₂ enabled the achievement of about 95% of the theoretical density. It is hence confirmed the very refractory nature of HfC and TaC, even when ultrafine powders (200–250 nm) are employed. The mechanical properties of the composites improved compared to the monoliths, due to the lower amount of residual porosity. Unreacted HfO₂ agglomerates were identified as critical flaws in the HfC-based materials, which, however, maintained nearly unaltered the flexural strength from room temperature to 1500 °C in Argon, around 300 for the monolith and around 400 for the composite. On the contrary, TaC-based ceramics showed a strength decrease at 1500 °C, due to the formation of Ta₂O₅ platelets and gaseous species which led to a collapse to 30–50% of the room temperature value, from around 600 to 300 MPa for the composite.

Acknowledgements

This work was carried out in the frame of the bilateral project between ISTEC-CNR (Italy) and SIC-CAS (China).

References

- Toth LE. Transition metal carbides and nitrides. In: Margrave JL, editor. *Refractory materials, a series of monographs*. New York: Academic Press Inc.; 1971. p. 6–10.
- Storms EK. The refractory carbides. In: Margrave JL, editor. *Refractory materials, a series of monographs*. New York: Academic Press Inc.; 1967. p. 94.
- Shvab SA, Egorov FF. Structure and some properties of sintered tantalum carbide. *Sov Powder Metall Metal Ceram* 1982;**21**:894–7.
- Samonov GV, Petrikina RY. Sintering of metals, carbides, and oxides by hot pressing. *Phys Sintering* 1970;**2**:1–20.
- Jackson JS. Hot pressing high-temperature compounds. *Powder Metall* 1961;**8**:73–100.
- Ramqvist L. Hot pressing of metallic carbides. *Powder Metall* 1966;**9**:26–46.
- Scholz S. Some new aspects of hot pressing of refractories. In: Popper P, editor. *Special ceramics*. New York: Academic Press Inc.; 1963. p. 293–307.
- Roeder E, Klerk M. Studies with the electron-beam microanalyzer on hot-pressed tantalum carbide having small additions of manganese and nickel. *Z Metallkunde* 1963;**54**:462–70.
- Zhang X, Hilmas GE, Fahrenholtz WG. Hot pressing of tantalum carbide with and without sintering additives. *J Am Ceram Soc* 2007;**90**:393–401.
- Zhang X, Hilmas GE, Fahrenholtz WG. Densification and mechanical properties of TaC-based ceramics. *Mater Sci Eng A* 2009;**501**:37–43.
- Opeka MM, Talmy IG, Wuchina Zaykoski JA, Causey SJ. Mechanical, thermal and oxidation properties of refractory hafnium and zirconium compounds. *J Eur Ceram Soc* 1999;**19**:2405–14.
- Wuchina EJ, Opeka MM, Causey SJ, Buesking K, Spain J, Cull A, et al. Designing for ultrahigh-temperature applications: the mechanical and thermal properties of HfB₂, HfC_x, HfN_x and αHf(N). *J Mater Sci* 2004;**39**:5939–49.
- Sciti D, Silvestroni L, Guicciardi S, Dalle Fabbriche D, Bellosi A. Processing, mechanical properties and oxidation behaviour of TaC and HfC composites containing 15 vol% TaSi₂ or MoSi₂. *J Mater Res* 2009;**24**:2056–65.
- Sciti D, Guicciardi S, Nygren M. Densification and mechanical behaviour of HfC and HfB₂ fabricated by spark plasma sintering. *J Am Ceram Soc* 2008;**91**:1433–40.
- Sciti D, Silvestroni L, Bellosi A. High density pressureless sintered HfC-based composites. *J Am Ceram Soc* 2006;**89**:2668–70.
- Liu JX, Kan YM, Zhang GJ. Synthesis of ultra-fine hafnium carbide powder and its pressureless sintering. *J Am Ceram Soc* 2010;**93**:980–6.
- Liu JX, Kan YM, Zhang GJ. Pressureless sintering of tantalum carbide ceramics without additives. *J Am Ceram Soc* 2010;**93**:370–3.
- Evans AG, Charles EA. Fracture toughness determination by indentation. *J Am Ceram Soc* 1976;**59**:371–2.
- Silvestroni L, Sciti D, Kling J, Lauterbach S, Kleebe HJ. Sintering mechanisms of zirconium and hafnium carbides doped with MoSi₂. *J Am Ceram Soc* 2009;**92**:1574–9.
- Baik S, Becher PF. Effect of oxygen contamination on densification of TiB₂. *J Am Ceram Soc* 1987;**70**:527–30.
- Sciti D, Vicens J, Herlin H, Grabis J, Bellosi A. SiC nanomaterials produced through liquid phase sintering: processing and properties. *J Ceram Proc Res* 2004;**5**:40–7.